

IMAGING OF AN ULTRASONIC WAVE REFLECTED BY AN OBJECT USING AN ACOUSTIC LENS IN AIR

Sai Hou, Buren Mandula, Wei Quan, Sahdev Kumar, Hideo Furuhashi

Department of Electrical and Electronics Engineering,
Faculty of Engineering
Aichi Institute of Technology
1247, Yachigusa, Yakusa-cho, Toyota, Aichi, Japan
furuhasi@aitech.ac.jp

Abstract – We have investigated the imaging of an ultrasonic wave reflected by an object using an acoustic lens in air. The reflected ultrasonic wave is focused by a spherical acoustic lens on an ultrasonic array sensor having 32 ultrasonic receivers. We have designed and manufactured the acoustic lens, which has a diameter of 25 cm. The imaging of the ultrasonic wave is demonstrated experimentally. This approach does not require delay-and-sum operation and can be operated using a small amount of memory. Therefore, load calculation is decreased.

Keywords: imaging, ultrasonic, array sensor, range sensor, acoustic lens

1. INTRODUCTION

Many different imaging sensor systems can obtain depth images in air. One approach to depth imaging involves the use of ultrasonic sensors. Ultrasonic sensors have a low probability of privacy violation and are simple to construct. Various ultrasonic depth imaging sensor systems that use arrays have been proposed [1, 2]. We have also reported an imaging sensor system that uses the spread spectrum method and a dispersed ultrasonic array [3-5].

Such depth imaging systems use delay-and-sum operations to produce an image electrically. To increase the resolution of the angle, many receivers are required. However, the increase in the number of receiver elements increases the amount of calculations, high speed operation, and increased memory is required. If the ultrasonic array sensor has receiver elements $n \times n$, the sampling time for the delay increases linearly with the number of elements by n . The sum operation increases linearly with the total number of elements by n^2 . Therefore, the calculation quantity increases by n^3 . The required memory address increases by n^2 , and the required bits for the data also increase with the increase of the sampling rate of the signal. Consequently, the load calculation of the electrical circuit increases significantly.

In this paper, depth imaging using an ultrasonic array sensor with an acoustic lens is discussed. This system does not require electrical imaging. The image is obtained acoustically. It does not need delay-and-sum operation and can be operated using a small amount of memory. The load calculation is smaller than that of a system using electrical imaging such as delay-and-sum operation. The characteristics

of the spherical acoustic lens in the system are discussed. The imaging of the ultrasonic wave is demonstrated experimentally.

2. METHOD

2.1. Acoustic lens

A reflection acoustic lens with a spherical surface was used. A schematic of the lens with the coordinate system is shown in Fig. 1. The origin of the coordinate system is the center of the surface of the lens. The lens has a radius of curvature R and a focal length of $f = R/2$. A plane acoustic wave having a directional vector $\vec{W} = (\tan \theta_x, \tan \theta_y, 1)$ focuses at the point $P = (p_x, p_y, p_z)$. Here

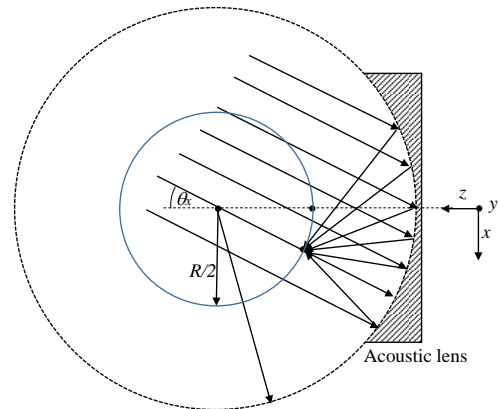


Fig.1. Focus point of the plane wave coming from the direction θ_x .

$$p_x = f \frac{\tan \theta_x}{\sqrt{(\tan \theta_x)^2 + (\tan \theta_y)^2 + 1}}$$

$$p_y = f \frac{\tan \theta_y}{\sqrt{(\tan \theta_x)^2 + (\tan \theta_y)^2 + 1}}$$

$$p_z = 2f - f \frac{1}{\sqrt{(\tan \theta_x)^2 + (\tan \theta_y)^2 + 1}} \quad (1)$$

Figure 2 shows the acoustic lens used in this experiment. It is made up of chemical wood having a diameter of 25 cm and a thickness of 85 mm. The radius of curvature is 20 cm. Therefore, the focal length is 10 cm, the angle of view is 51°, and the numerical aperture, NA , is 0.78. The resolution of the lens is calculated as follows:

$$\delta = \frac{0.61 \times \lambda}{NA} = \frac{0.61 \times 8.6 \text{ mm}}{0.78} = 6.7 \text{ mm}, \quad (2)$$

where λ is the wavelength of the ultrasonic wave at 40 kHz. The focal depth d is obtained as follows:

$$d = \frac{\lambda}{NA^2} = \frac{8.6 \text{ mm}}{0.78^2} = 14 \text{ mm}. \quad (3)$$

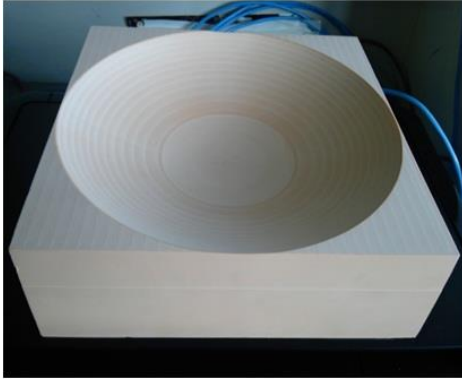


Fig.2. Acoustic lens.

2.2. Ultrasonic array receiver

The arrangement of the ultrasonic sensor elements of the ultrasonic array sensor used in this experiment is shown in Fig. 3. It consists of 32 receivers (Knowledge Acoustics SP0103NC3-3, 6.15 mm × 3.76 mm). The locations of the receivers are shown in Table 1. The minimum interval of the elements is 4.2 mm, which is smaller than the resolution of the lens (6.7 mm) as shown in equation (2).

The array sensor is located in front of the acoustic lens with a focal length of 10 cm. The focal point of the lens for the plane wave coming from the front of the lens is set to the No. 1 element position. The position having the maximum distance from the No. 1 element (15.3 mm, -8.4 mm) is at the No. 25 element. The size of the array is 26.4 mm × 26.4 mm. The board has an external size of 60 mm × 60 mm.

Since the z axis of all the elements on the array sensor is $z = 10$ cm, the focus point for the plane wave, for which the incident angle to the lens is not 0, is not on the sensor. The approximate focus point on the array sensor (a_x, a_y, f) is given as follows.

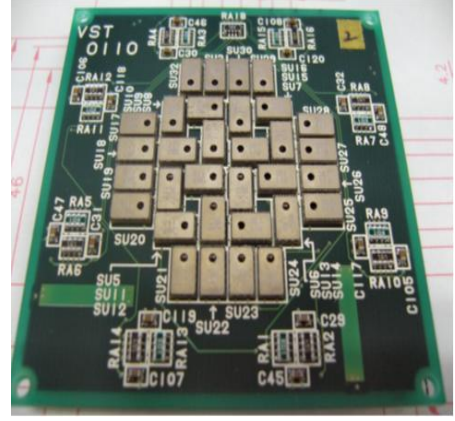


Fig.3. Ultrasonic array sensor.

Table 1. Position of the receivers (mm).

No.	x	y	No.	x	y
1	0	0	17	-11.1	4.2
2	0	-4.2	18	-11.1	0
3	4.2	-4.2	19	-11.1	-4.2
4	4.2	0	20	-11.1	-8.4
5	-4.2	0	21	-4.2	-15.3
6	0	-8.4	22	0	-15.3
7	8.4	-4.2	23	4.2	-15.3
8	4.2	4.2	24	8.4	-15.3
9	0	6.9	25	15.3	-8.4
10	-6.9	4.2	26	15.3	-4.2
11	-6.9	4.2	27	15.3	0
12	-4.2	-11.1	28	15.3	4.2
13	4.2	-11.1	29	8.4	11.1
14	11.1	-8.4	30	4.2	11.1
15	11.1	0	31	0	11.1
16	8.4	6.9	32	-4.2	11.1

$$\begin{aligned} a_x &= f \tan \theta_x \\ a_y &= f \tan \theta_y \end{aligned} \quad (4)$$

The error of the focus point position Δf by the approximation is given as follows.

$$\begin{aligned} \Delta f &= \sqrt{(a_x - p_x)^2 + (a_y - p_y)^2 + (a_y - p_y)^2} \\ &= f \left(\sqrt{(\tan \theta_x)^2 + (\tan \theta_y)^2 + 1} - 1 \right) \end{aligned} \quad (5)$$

The maximum error is that of the No. 25 element. At 1.1 mm, this error is smaller than the focal depth of 14 mm obtained by equation 3. Therefore, the aberration of the spherical lens is negligible.

Since the array sensor has a size of 26.4 mm × 26.4 mm, the view angle (θ_x, θ_y) (full angle) of the sensor is approximated as

$$\theta_x = \theta_y \approx 2 \tan^{-1} \frac{26.4 \text{ mm}}{2f} = 15^\circ. \quad (6)$$

The incident ultrasonic wave is partly obstructed by the array sensor board. This obstruction is estimated as

$$\frac{60^2}{\pi \times 125^2} = 7.3\%. \quad (7)$$

The influence of the board is small and, as a result, a large signal will be obtained from the acoustic lens.

3. EXPERIMENTAL PROCEDURE

Figure 4 shows the experimental setup. A single transmitter (Murata Manufacturing MA40S4S) was used to produce an ultrasonic wave of 40 kHz. The wave was modulated by a pulse with a half width of 0.4 ms at intervals of 40 ms. It was located at a distance of 40 cm from the acoustic lens. An object was located 300 cm away from the acoustic lens and its position was changed horizontally. That is, $\theta_y = 0^\circ$ only θ_x was changed.

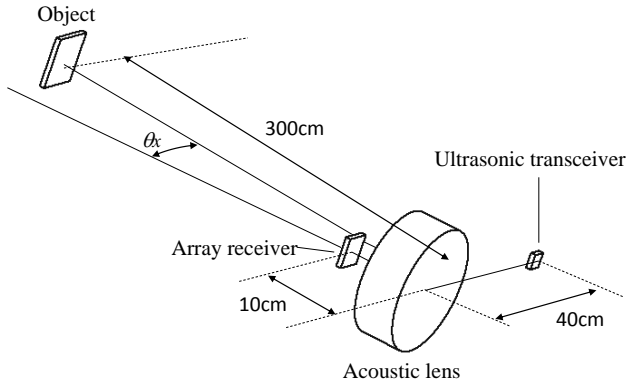


Fig.4. Experimental setup.

The resolution of the distance is calculated to be

$$0.4 \text{ ms} \times 345 \text{ m} \div 2 = 69 \text{ mm}. \quad (8)$$

Here, the acoustic velocity is 345 m. The resolution of lens is smaller than the measurement resolution of the distance based on the pulse width. The measurable range of the distance is

$$40 \text{ ms} \times 345 \text{ m} \div 2 - 10 \text{ cm} = 6.8 \text{ m}. \quad (9)$$

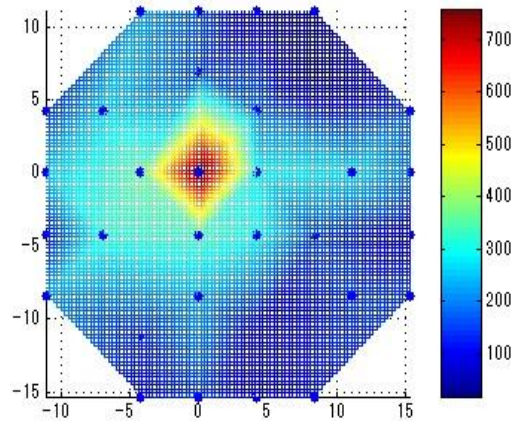
This value is longer than the distance of the object.

The received ultrasonic signals are measured by AD converters with a sampling rate of 2.5 μs after the trigger signal from the ultrasonic transceiver. These signals are then fed into a computer. The peak amplitude of each signal was calculated with the dead time of 3 ms. The received time of the direct signal from the transceiver is calculated to be

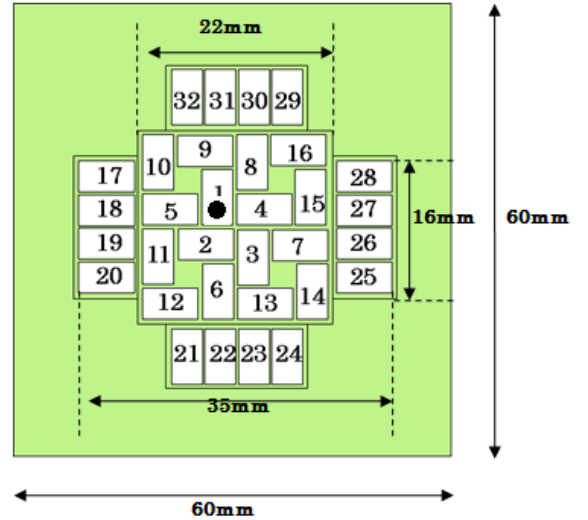
$$40 \text{ cm} \div 345 \text{ m} = 1.16 \text{ ms}. \quad (10)$$

Therefore, the direct signal is ignored.

Figure 5(a) shows the detected ultrasonic signal amplitude when the object is located at $\theta_x = 0^\circ$. The dots in the figure show the points at which the ultrasonic receiver is located. The signal between each element is spatially interpolated. The arrangement of the ultrasonic receiver elements is also shown in Fig. 5(b), and the dot is the point at which receiver No. 1 receives sound.

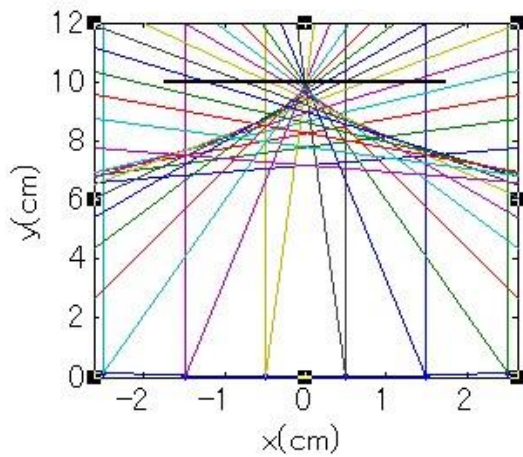


(a) Signal amplitude.



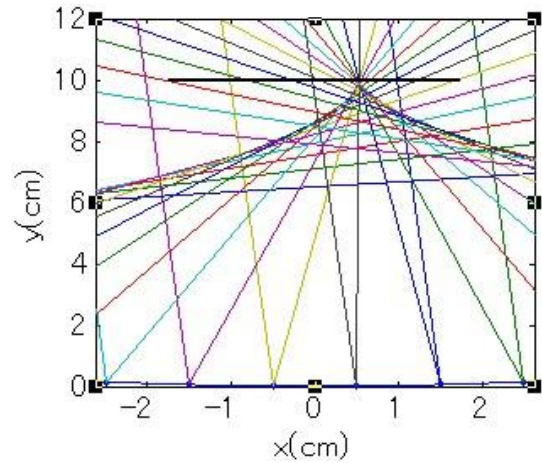
(b) Arrangement of the receiver elements.

The dot is the point at which receiver No. 1 receives sound.



(c) Simulated focusing.

Fig.5. Signal amplitude, position of the elements, and simulated focusing for $\theta_x = 0^\circ$.



(b) Simulated focusing.

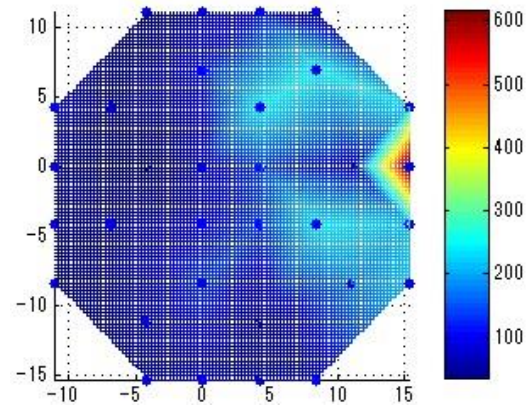
Fig.6. Signal amplitude and simulated focusing for $\theta_x = 3^\circ$.

The time peak signal was detected by receiver No 1 after the trigger from the ultrasonic transceiver was measured, which was about 17.8 ms. The distance of the object is calculated to be

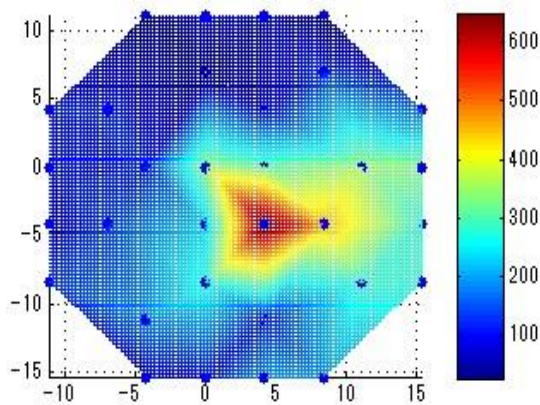
$$17.8 \text{ ms} \times 345 \text{ m} \div 2 - 10 \text{ cm} = 3.06 \text{ m.} \quad (11)$$

The measurement resolution of the distance is 0.069 m. Therefore, the calculated distance of the object is correct in the range of the resolution

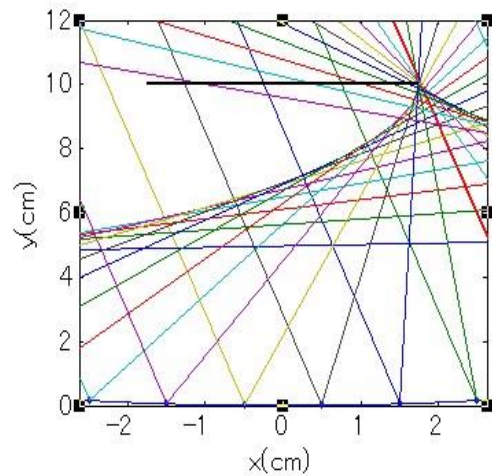
Figures 6 and 7 show the detected ultrasonic amplitude when the object is located at $\theta_x = 3^\circ$ and 9° along with the respective simulated focusing. The approximate focus points are calculated to be 5.2 and 15.8 mm, respectively, using equation 4.



(a) Signal amplitude.



(a) Signal amplitude.



(b) Simulated focusing.

Fig.7. Signal amplitude and simulated focusing for $\theta_x = 9^\circ$.

Although the theoretical focus point is the No. 4 element (4.2 mm, 0 mm) for the case of $\theta_x = 3^\circ$, the actual focus is on the No. 3 element (4.2 mm, -4.2 mm). The difference of the y axis is within the error margin of the object setting.

The theoretical focus point is the No. 27 element (15.3 mm, 0 mm) for the case of $\theta_x = 9^\circ$.

4. CONCLUSIONS

We have investigated the imaging of an ultrasonic wave reflected by an object using an acoustic lens in air. A reflection spherical acoustic lens has been designed and manufactured. This approach does not require delay-and-sum operation and can be operated using a small amount of memory. The imaging of the ultrasonic wave has been demonstrated experimentally.

5. ACKNOWLEDGMENT

This work was supported by MEXT KAKENHI Grant Number 15K05879.

REFERENCES

- [1] P. N. Keating, T. Sawatari and G. Zilinskas, "Signal Processing in Acoustic Imaging," *Proceedings of the IEEE*, Vol.67, pp.496-510, 1979.
- [2] L. J. Griffiths and K. M. Buckley, "Quiescent Pattern Control in Linearly Constrained Adaptive Arrays," *IEEE Trans. Acoustic, Speech and Signal Processing*, Vol.ASSP-35, pp.917-926, 1987.
- [3] H. Furuhashi, J. Valle, Y. Uchida and M. Shimizu, "Imaging Sensor System using Dispersed Ultrasonic Array," *Proceedings of the ICCAS 2007*, Vol. FEP-35, 2007.
- [4] H. Furuhashi, Y. Uchida and M. Shimizu, "Imaging Sensor System using Composite ultrasonic Array," *Proceedings of IEEE Sensors 2009*, pp. 1467-1472, 2009.
- [5] H. Furuhashi, S. Kumar and M. Shimizu, "Signal Processing of a 3D Ultrasonic Imaging Sensor that uses the Spread Spectrum Pulse Compression Technique," *Lecture Notes in Information Technology*, Vol.14, pp.145-150, 2012